JOURNAL OF OPTOELECTRONICS AND ADVANCED MATERIALS Vol. 9, No. 11, November 2007, p. 3499 - 3504

Diffractive optics for spatial and temporal analysis of pollution in liquid media

M. MIHAILESCU[a*], A. M. PREDA[a], A. SOBETKII[b], E. I. SCARLAT[a], L. PREDA[a]
[a]*Physics Department, University "Politehnica" of Bucharest, Romania*
[b]*OPTICOAT SRL, Bucharest, Romania*

We designed some diffractive optical elements (DOEs) in order to utilize them in optoelectronics setups to establish spatial and temporal optical path variations of pollution in liquid media. In the design algorithm, besides classical parameters (the diffraction efficiency, the contrast in desired spots, the wavelength, the divergence angle of every desired spots), we optimized the diffractive pattern to have information in the same time from many fixed points of the investigated volume. We analyzed different experimental setups with diffractive beam splitter and we selected the suitable optoelectronic components for each investigated liquid sample. Our setups permit measurements of the optical path variations due to geometrical path variations or refractive index variations. Changes in concentrations or in chemical composition of the sample induce refractive index gradients and the intensity distribution in diffractive patterns is modified. The monitoring of the spatial and temporal changes in diffractive pattern was done with CCD and processed on the computer. To calibrate our method, we utilized some mixtures of water-glucose or water-$CuSO_4$ in known percentages. Our results are complementary with those obtained with classical physical-chemical analysis and permit automated spatial and temporal monitoring of the polluted liquid media in big volumes.

(Received August 1, 2007; accepted November 1, 2007)

Keywords: diffractive optical element, pollution, liquid media, refractive index

1. Introduction

Modern techniques in experimental determination of liquids properties are based on opto-electronic measurements, because they are simple, non-destructive and are attractive for sensing applications in hostile environments. Besides classical optical methods: reflectrometry [1], interferometry [2], in the past years were used in many setups new methods based on diffraction with digital processing of images: diffractometer for living cells in aqueous media [3], digital holography [4], digital holographic interferometry [5].

Also, in many areas of industry and in the environment pollution are requirements for high-speed automatic inspection of two-dimensional pattern for the rapid gauging of small components. The classical visual inspection is relatively slow and the cost of labor is high, especially where detailed microscopic examination is required. There is, therefore, a need for an optoelectronic technique that can inspect for, and possible classify a wide range of defects at high speed. A new digital technique is, at present, under development, which is suitable for inspection of objects having complex shapes or patterns. This method, which uses a laser source and micro-opto-electro-mechanical systems (MOEMS), involves Fourier analysis of the intensity of diffracted, scattered of light or specularly transmitted (or reflected) from the object. Selected components of the Fourier transform of a reference pattern are compared at high speed with corresponding signals for the pattern under test, and small differences in geometry and the structure of the two objects are shown.

The analysis and modeling of refractive index distribution in liquid media and their influence in mass transfer are interesting in environmental physics. In order to understand the mass transfer on liquid boundaries it is highly desirable to know the refractive index profile at these boundaries. We propose a system which uses the image on screen of the regular structure of the DOE in order to monitor the spatial and temporal changes in refractive index of a liquid sample inserted in an experimental cell (LC). Previously, for some alimentary colorants complex refractive indices measurements, was used a DOE sensor, but there the image on screen was the diffractive pattern from DOE [6]. Sensors based on DOE are used also for: number density of 8μm droplets suspension in liquid [7], local inspections of fine paper [8], two-dimensional map of optical properties of metallic surfaces [9]. Also a new LIDAR systems use a DOE incorporating to scan different points of the atmosphere in the same time [10].

2. Theory

A diffractive optical element (DOE) is a micro-optical component, which has a calculated micro-structure to modulate the incident wave in phase and/or in amplitude with the aim to obtain a desired diffractive image in far-field or near-field, in concordance with the desired application.

We designed DOE with a variant of an Iterative Fourier Transform Algorithm (IFTA). We started with the image which we want to form after DOE, like a matrix in MATLAB with M_x, M_y elements where we delimitated a signal window with the desired spots. At the end of the algorithm we find another matrix which represents the mathematical description of the DOE structure. We did the description of the algorithm elsewhere [11]. Our previous simulations have the aim to change the parameters of the algorithm and to find the better variants for DOE structure which forms the desired spots with maximum efficiency and minimum contrast inside (all the pixels must have the same intensity or nearer values) [12].

In this paper we started with a given DOE with transmission function $t(m_x\Delta x, m_y\Delta y)$ determinate at the end of the IFTA. We worked with discrete functions and coordinate in MATLAB, where $m_x = 1,...,M_x, m_y = 1,...M_y$ and $\Delta x, \Delta y$ are the dimensions of the pixels in both directions in DOE plane. The dimensions of the pixels in another plane, parallel with the DOE plane, at a given distance z_1 are $\Delta\tilde{x}, \Delta\tilde{y}$ and the relations between them are [13]:

$$M_1\Delta x\Delta\tilde{x} = \lambda z_1 \text{ and } M_2\Delta y\Delta\tilde{y} = \lambda z_1 \quad (1)$$

If we consider a monochromatic plane wave with unit amplitude, normally incident on the DOE, then the field distribution immediately after DOE is [14]:

$$g(m_x\Delta x, m_y\Delta y) = t(m_x\Delta x, m_y\Delta y) \quad (2)$$

The field distribution $\tilde{g}(\tilde{m}_x\Delta\tilde{x}, \tilde{m}_y\Delta\tilde{y})$ at a given distance z_1 is given by:

$$\tilde{g}(\tilde{m}_x\Delta\tilde{x}, \tilde{m}_y\Delta\tilde{y}) = \frac{\exp(ikz)\exp\left[i\frac{k}{2z}\left((\tilde{m}_x\Delta\tilde{x})^2 + (\tilde{m}_y\Delta\tilde{y})^2\right)\right]}{iz\lambda} \cdot \text{FFT2}\left\{t\left(m_x\Delta x, m_y\Delta y\right)\right\} \quad (3)$$

where FFT2 is a bi-dimensional fast Fourier transform implemented in MATLAB.

Its squared value in every pixel, gives us the intensity distribution according to the desired image after DOE. We know from Fourier optics theory that a lens makes a Fourier transform of the incident distribution. If we put a lens after DOE, then in far field will be form on the screen the image of the DOE structure. If we put a liquid cell (LC) with different composition between DOE and lens, we obtain on the screen an image which preserves the DOE structure but also contains information about the complex refractive indices of the LC. We named this – „dusty" DOE structure (DDOES).

The intensity distribution after DOE is incident on liquid cell. We can say that the LC is an optical element, which has a bi-dimensional complex refractive indices distribution. It acts like a transmission function, t_a, which modulates also the amplitude, χ ,and the phase:

$$\tilde{t}_a(\tilde{m}_x\Delta\tilde{x}, \tilde{m}_y\Delta\tilde{y}) = \chi(\tilde{m}_x\Delta\tilde{x}, \tilde{m}_y\Delta\tilde{y}) \exp\left[\frac{2i\pi}{\lambda}\left(n(\tilde{m}_x\Delta\tilde{x}, \tilde{m}_y\Delta\tilde{y})h\right)\right] \quad (4)$$

where *h* is the thickness of the LC. The angular spectrum of the field immediately after LC is obtain in theory by convolution between the angular spectrum of the incident wave and the angular spectrum specific of the LC. If we apply the convolution theorem [15], we obtain the field distribution immediately after LC:

$$t'(\tilde{m}_x\Delta\tilde{x}, \tilde{m}_y\Delta\tilde{y}) = \tilde{t}_a(\tilde{m}_x\Delta\tilde{x}, \tilde{m}_y\Delta\tilde{y}) \cdot \cdot \tilde{g}(\tilde{m}_x\Delta\tilde{x}, \tilde{m}_y\Delta\tilde{y}) \quad (5)$$

And after lens we have the intensity distribution given by:

$$\left|\tilde{\tilde{t}}(\tilde{\tilde{m}}_x\Delta\tilde{\tilde{x}}, \tilde{\tilde{m}}_y\Delta\tilde{\tilde{y}})\right|^2 = \left|FFT2\left(t'(\tilde{m}_x\Delta\tilde{x}, \tilde{m}_y\Delta\tilde{y})\right)\right|^2 \quad (6)$$

which preserves the information also about the LC and the DOE structure.

3. Simulation procedure

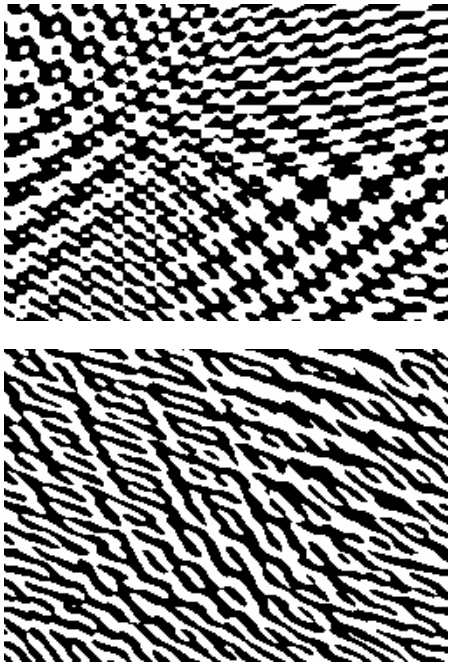

Fig. 1a. The image of DOE structure beore lens.

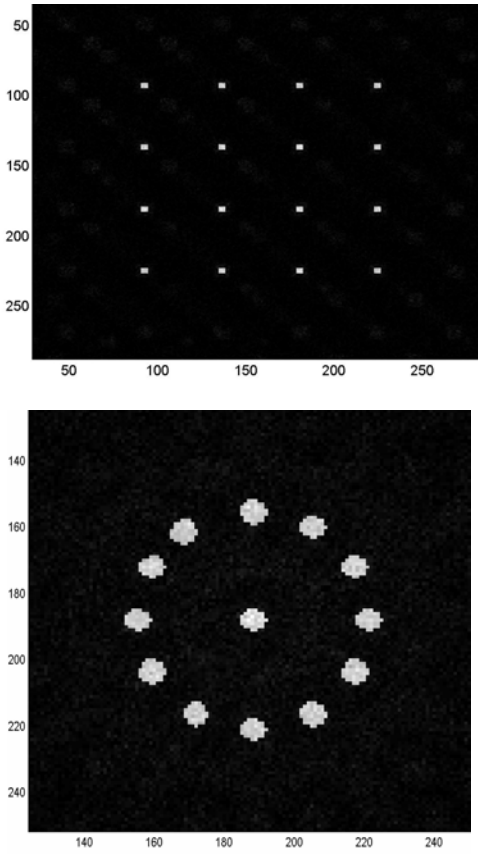

Fig. 1b. The diffractive patterns obtained with the structures from Fig. 1a. On the axis are the pixel numbers.

In Fig. 1 we present two examples of DOE structures funded with IFTA $t(m_x\Delta x, m_y\Delta y)$ and their desired images produced in signal window like a diffractive pattern $\tilde{g}(\tilde{m}_x\Delta\tilde{x}, \tilde{m}_y\Delta\tilde{y})$ incident on LC.

We selected for our simulations four cases to describe mathematically the transmission function of the liquid cell which has a bi-dimensional distribution of the complex refractive index: (1) the transmission function of the inhomogeneous LC with a linear variation both in amplitude and phase from bottom to top; (2) the transmission function of the inhomogeneous LC with a graded step-like variation both in amplitude and phase; (3) the transmission function of the inhomogeneous LC with a graded step-like variation only in amplitude and constant phase; (4) the transmission function of the inhomogeneous LC with a graded step-like variation only in phase and constant amplitude.

We can see in Fig. 2 by comparison with Fig. 1a, that we obtain the „dusty" DOE structure. Each simulation case of the inhomogeneous LC transmission function modifies in different form the DOE structure. In all these cases we cut and enlarge the same portion of the DOE structure.

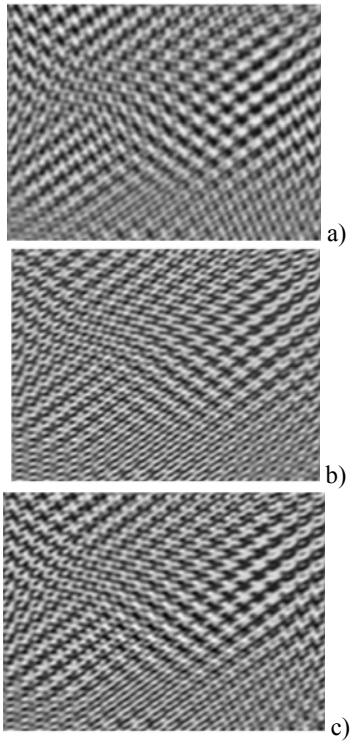

Fig. 2. The images of the DOE structure after lens when the transmission function of the LC has: a) linear variation both in amplitude and phase; b) graded step-like variation only in amplitude and constant phase; c) graded step-like variation only in phase and constant amplitude.

We compare the reference image of the DOE structure, which may obtain on the screen without LC, with the image of the altered structure of the DOE when in experimental setup was inserted the inhomogeneous LC. We made separately differences, ratio of the real part, or of the amplitude, or of the phase between reference image of the DOE structure and the altered one. Better results were obtained when we simulated the back propagation in $\left(\tilde{m}_x\Delta\tilde{x}, \tilde{m}_y\Delta\tilde{y}\right)$ plane, started with an image with altered structure of the DOE, using the inverse bi-dimensional Fourier transform (IFFT2). In this case, we reconstruct the desired image from DOE, but affected by the bi-dimensional distribution of the transmission function of the liquid cell (Fig. 3).

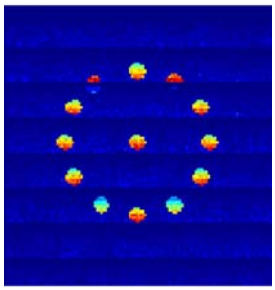

Fig. 3. The image obtained through back propagation starting with a simulated one.

We can easily observe that in Fig. 3 the desired spots are modulated also in intensity in function by the inhomogeneity of the liquid, besides the Fig. 1 where the spots are uniform. We used the same procedure in different simulated situation and also when we started with experimental images recorded on CCD.

4. Experimental results

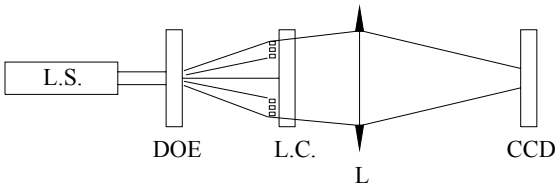

Fig. 4. The sketch of the experimental setup: L.S. laser; L.C. liquid cell; L lens.

In experimental setup (Fig. 4), we used a laser (HeNe), a DOE which forms a diffractive pattern with a shape as in Fig. 1, incident on a cell which contained a liquid. The resulted image-diffractive pattern is formed in far field on the CCD. In Fig. 5 are two images obtained experimentally from the DOE with the structure presented in Fig. 1. In our experimental arrangement these intensity distributions are incident on the LC (not simultaneous).

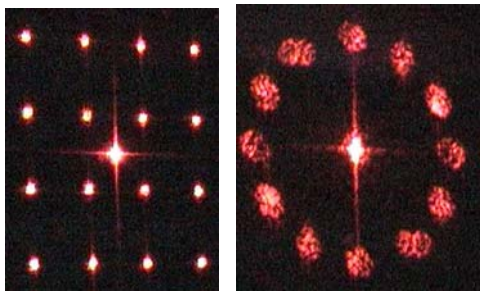

Fig. 5 The intensity distribution in diffraction pattern after DOE, incident on LC.

To obtain DOE, after we chose the parameter of the IFTA, we tested our structure of the DOE on a spatial light modulator (SLM). It is a two-dimensional electrically addressable device, which modulates the phase and/or amplitude of the incident wavefront by a spatial variation in the optical path length by controllable changes in refractive index of the twist nematic liquid crystal cells, according with the image addressed from the computer. The generation of an individual pixel well-controlled phase and amplitude distribution in real time is a property of the SLM, which we used to test our DOE design, because their fabrication on glass is expensive and time consuming. Then, the best structures are used to fabricate DOE in glass with a technique based on e-beam writing. The DOE which we used in our experiment is an amplitude one and the processes involved in technological procedure is schematic described in Fig. 6.

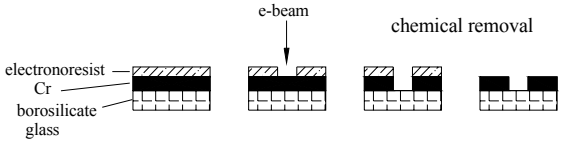

Fig. 6. Processes involved in DOE fabrication

We used different DOE structure and we chose those which fulfill some resolution requirements: (1) the diffractive pattern must not be larger than aperture of the LC. This isn't a requirement if we study the liquid in natural environment; (2) the minimum dimension of DOE structure must be 3μm to form in CCD plane an image which has the minimum size bigger than of the pixel size in sensor array for our Sony, DCR-TRV140E.

The images recorded on CCD are like the simulated one from Fig. 2, with the "dusty" structure of the DOE, preserving the information from the LC. These are processed in a similar manner like in simulation section. Starting with these images (Fig. 7) we must reconstruct the spatial distribution in LC plane.

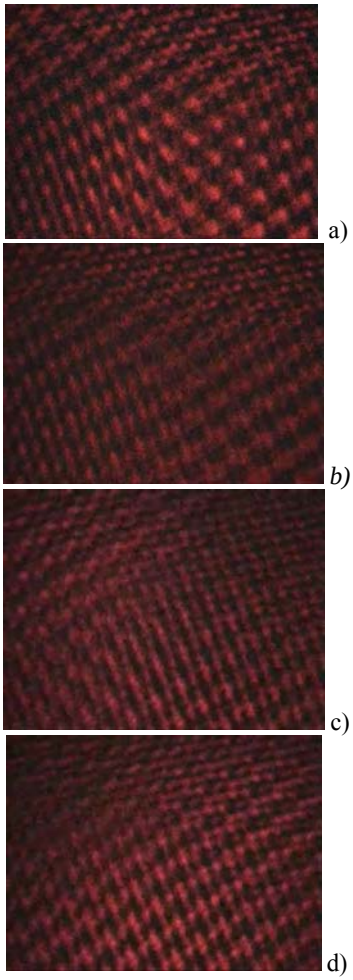

Fig. 7. Images on CCD of the DOE structure with homogeneous LC a); and inhomogeneous LC b), c), d) at different moments.

If we make our observations during the time, we record a series of images (Fig. 7b, c, d), which has small differences from one to the other, in different points (not in all plane). When we processed these series we had information about the temporal evolution of the complex refractive indices and implicitly about the motion of the inhomogeneity. We processed image from two consecutive frames of our CCD which work at 25frames/s.

These images are different also in intensity, so we can determine the transmittance of the liquid $T = I / I_0$ where I_0 is the value of the intensity in the image on CCD with homogeneous LC in experimental setup and I with inhomogeneous LC. The absorbance of the liquid in each point is given by $A = -\ln \frac{I}{I_0}$ [6]. Also the transmission and the absorbance are a bi-dimensional map, because we started with the image recorded on the CCD.

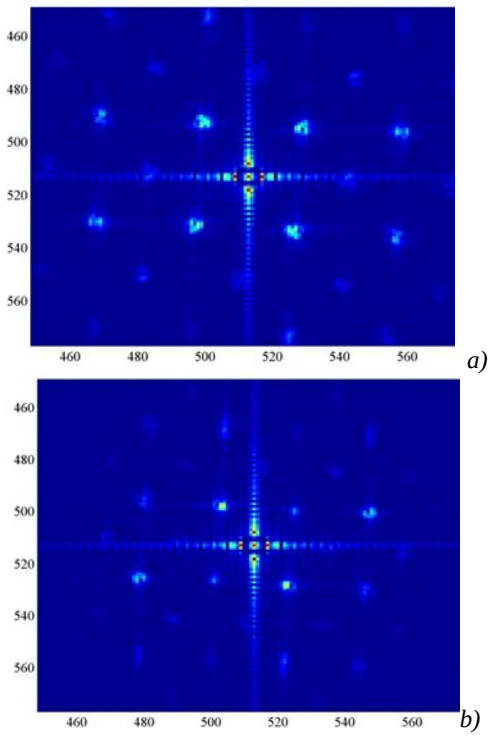

Fig. 8. The images obtained through back propagation starting with an experimental one when in cell exist only water a) or water with refractive index gradient of 10^{-2}/cm b) Numbers shown on the axis are the pixel numbers.

We can see in Fig. 8, that the intensity distribution after simulated back propagation, starting with the image with homogeneous LC (a) and inhomogeneous LC (b) are different. The position of the local maxima are different and also their value. To have a quantitative measure of the displacement introduced by the complex refractive indices variations, we make the differences between these two images (Fig. 9).

The black spots in Fig. 9 correspond to homogeneous LC and the white spots to inhomogeneous LC. The distances between these two kinds of spots at high spatial frequency are smaller than at the low spatial frequency. The white spots from the edges aren't square, but they have an elongated shape. Here appear the advantages to utilize a DOE, which splits the laser beam in a desired spatial distribution of several spots, which pick up information from many points of the LC, besides the utilization of a single laser beam. If we want to collect information from many points or from large area we must start the designed algorithm (IFTA) from the other desired images.

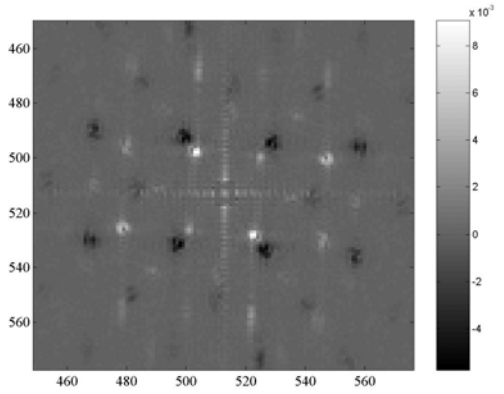

Fig. 9. The differences between images in LC plane when we have homogeneous liquid (black points) and inhomogeneous liquid (white points)

We calibrate the method using some homogeneous liquid with different refractive indices measured with Abbe refractometer, prepared in a known percentage of water and glucose. To make a correspondence between the displacement of the spots and the refractive index we used the theory based on optical path length and angle deviation presented in [16].

The displacements of the white spots from Fig. 9 are putting in relations with the value of the refractive indices of the prepared solutions. Displacement of the black spots besides white spots, with different values in different regions, indicates a different value for refractive index in that region. These results are compared with the images resulted for inhomogeneous sample, with a sugar crystal in the center of the cell, on the bottom. The variations of the refractive indices was at the order of 10^{-2} verify with Abbe refractometer, from center to edges.

5. Conclusions

Due to fast specialized algorithms and improvements in computer memory and processor, we can design rapidly any DOE, even if the desired image is complicated. Also the micro scale production techniques with e-beam lithography ensure very well fabrication of the DOE structure given at the end of the algorithm. Therefore, a sensor with DOE incorporated satisfies all requirements for a quality one, in resolution and uniformity in desired

spots. To implement it in opto-electronic techniques for monitoring changes in complex refractive indices, we also need a high-speed CCD. The recorded images can be displayed on a monitor in near real time and their processing also takes few minutes.

We demonstrated from simulation, that the back propagation from the image of the "dusty" DOE structure, gives us also the diffractive pattern and the transmission function of the LC (Fig. 3). We follow the same procedure starting with the image recorded on CCD in experimental process.

The simulated back propagation from the images when in experimental setup exists a homogeneous LC and inhomogeneous LC, show us the difference between these cases. The position of the local maxima are different and also their value. To have a quantitative measure of the displacement introduced by the complex refractive indices variations, we make the differences between two images (Fig. 9).

To make a correspondence between refractive index and displacements of the spots, we used some liquids with known refractive index and a theory based on optical path length and angle deviation.

We observe a deviation of the spots due to changes in refractive index of 10^{-2}. So, our method is sensitive, but the calibration must be done for each liquid component separately.

Our future aim is to design a DOE with a larger desired spots to pick up information from a larger area of the LC, and which has a minimum contrast in desired spots. Our method must also be calibrated for different samples.

References

[1] G. H. Meeten, A. N. North, Meas. Sci. Technol. **6**, 214, (1995).
[2] D. W. Watt, C. M. Vest, Experiments in Fluids **5**,401-406 (1987).
[3] Z. Ulanowski, R. S. Greenaway, P. H. Kaye, I. K. Ludlow, Meas. Sci. Technol. **13** 292, (2002)
[4] J. Garcia-Sucerquia, W. Xu, S. K. Jericho, P. Klages, M. H. Jericho, H. Jürgen Kreuzer, Appl. Opt. **45**, 836 (2006).
[5] A. Anand, V. K. Chhaniwal, C. S. Narayanamurthy, 904 APPL. OPT. Vol. **45**(5), 10 (2006).
[6] A. Jääskeläinen, R. Silvennoinen, K.-E. Peiponen, J. Räty, Opt. Comm. **178**, 53-57, (2000)
[7] F. Peters, A. Graßmann, H. Schimmel, B. Kley, Experiments in Fluids 35, 4 (2003).
[8] A. Oksman, R. Silvennoinen, K.E. Peiponen, M. Avikainen, H. Komulainen, Opto-electronics Rev. **13**(1), 39 (2005).
[9] K. Myller, K.-E. Peiponen, R. Silvennoinen, Opt. Eng., **42**(11), 3194 (2003).
[10] G. Schwemmer, "Shared Aperture Diffractive Optical Element Multiplexed Telescope" esto.nasa.gov/conferences/ESTC2006/papers/b9p2.pdf
[11] M. Mihailescu, A.M. Preda, D. Cojoc, E. Scarlat, L. Preda, J. Optoelectron. Adv. Mater. **9**(4), 1071 (2007).
[12] M. Mihailescu, A. M. Preda, E.I. Scarlat, L. Preda, U. P. B. Sci. Bull. A, **67**(4), 65 (2005).
[13] J. W. Goodman, "Introduction to Fourier optics", Mc Graw-Hill Book Company, 1968.
[14] J. Garcia, D. Mas, R. G. Dorsch, Appl. Opt. **35**(35), 7013 (1996).
[15] D. C. O'Shea, T. J. Suleski, A. D. Kathman, D. W. Prather, "Diffractive Optics - Design, Fabrication, and Test", Spie Press, Bellingham, Washington, USA, 2004;
[16] A. M. Preda, E. I. Scarlat, L. Preda, M. Mihailescu, Univ. Pol. of Buc. Sci. Bull. series A: Applied Mathematics and Physics **64**(2), 45 (2002).

*Corresponding author: mona_m@physics.pub.ro